Hexasilabenzene

DOI: 10.1002/anie.201209906

An Experimental Charge Density Study of Two Isomers of Hexasilabenzene**

*Daniel Kratzert, Dirk Leusser, Julian J. Holstein, Birger Dittrich, Kai Abersfelder, David Scheschkewitz, and Dietmar Stalke**

Dedicated to Prof. Manfred Weidenbruch on the occasion of his 75th birthday

The similarities and differences between carbon and its heavier congener silicon generate challenging synthetic targets, especially when multiply bonded systems are concerned. The first stable compound with a Si=Si bond goes back to West et al. in 1981,[1] and conjugated systems with Si=Si double bonds were pioneered in 1997 by Weidenbruch et al.[2] Whether silicon analogues of benzene can show aromatic character is still a point of constant debate.[3] The aromatic nature of silabenzenes has been predicted theoretically,[4] but the synthesis of a stable silabenzene was not accomplished until Tokitoh et al. reported the sterically encumbered 2,4,6-tris[bis(trimethylsilyl)methyl]phenyl-substituted monosila derivative.[5] At the same time, Ando et al. independently reported the synthesis of 1,4-disila Dewar benzene.[6] Only two years later, Sekiguchi et al. accomplished the synthesis of 1,2-disilabenzene by reacting RSi≡SiR (R = $Si(CH(SiMe_3)_2)iPr$) with PhC≡CH in a formal [2+2+2] cycloaddition reaction.[7] Recently, in a cooperative effort with the Roesky group, we reported the synthesis of a 1,4-disilabenzene by reacting $[\{PhC(NtBu)_2\}Si]_2$ with diphenyl alkyne.[8] With regards to homonuclear systems, the Scheschkewitz group recently made groundbreaking progress with the isolation of ring[9] and cage[10] isomers of hexasilabenzene (Scheme 1), which prompted the present experimental charge-density study.

The dark-green-colored six-membered ring system **1** rearranges upon heating or UV irradiation to the red silicon cage compound **2** with a bridged propellane structure.[10] An analogous transformation for fully saturated silicon compounds under irradiative conditions has been described by Kira and co-workers.[11] We propose a transition of **1** to **2** by the reaction pathway in Scheme 1 (bottom). The transformation proceeds by the breaking of the Si1–Si3 and Si2–Si4 bonds in **1**, followed by a twist of the four-membered silicon ring and the formation of the new Si1–Si2 and Si3–Si4 bonds (see Scheme 1 and video in the Supporting Information).

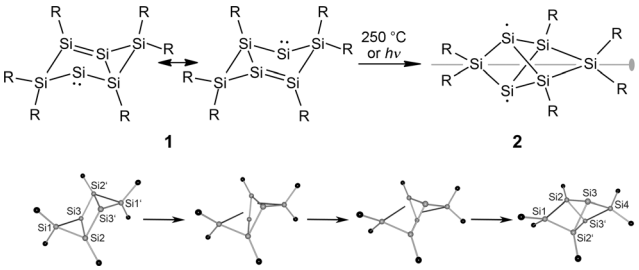

Scheme 1. The two hexasilabenzene isomers (R = Tip, 2,4,6-triisopropylphenyl) and the proposed transformation.

In the following, we analyze the bonding situation in the ring (**1**) and cage (**2**) isomer of hexasilabenzene $(TipSi)_6$ on the basis of experimental charge-density investigations (Figure 1). High-resolution X-ray data with $(\sin\theta/\lambda)_{max}$ = 1.11 for **1** and 1.16 $Å^{-1}$ for **2** were collected on a rotating anode diffractometer at 100 K, and the structures were refined using the Hansen and Coppens multipole model.[12] Subsequently, the resulting experimental charge-density (CD) distribution $\rho(\mathbf{r})$ was analyzed by topological analysis according to Bader's quantum theory of atoms in molecules (QTAIM).[13] Within this formalism, the topological properties of the density at a (3, −1) critical point, that is, a bond critical point (BCP), in the electron density distribution $\rho(\mathbf{r})$ between a pair of atoms describe character and strength of a chemical bond. Localization of $\rho(\mathbf{r})$ in the bonding region

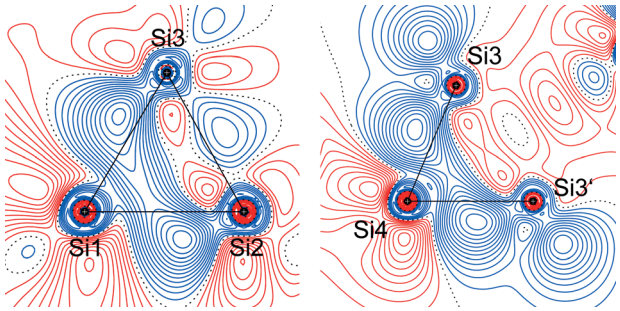

Figure 1. Static deformation density contour plot of **1** (left) and **2** (right). Contour lines are drawn at ±0.015, 0.03, ... e$Å^{-3}$ interval levels. Blue: positive; red: negative.

[*] D. Kratzert, Dr. D. Leusser, Dr. J. J. Holstein, Dr. B. Dittrich, Prof. Dr. D. Stalke
Institut für Anorganische Chemie der Universität Göttingen
Tammannstrasse 4, 7077 Göttingen (Germany)
E-mail: dstalke@chemie.uni-goettingen.de
K. Abersfelder, Prof. Dr. D. Scheschkewitz
Lehrstuhl für Allgemeine und Anorganische Chemie
Universität des Saarlandes, 66125 Saarbrücken (Germany)

[**] We kindly acknowledge funding from the DFG Priority Programme 1178 ("Experimental Electron Density as a Key to Understand Chemical Interactions") and the CMC.

Supporting information for this article is available on the WWW under http://dx.doi.org/10.1002/anie.201209906.

between the nuclei reaches a local minimum along the bond path at $\rho(\mathbf{r}_{BCP})$ (Figure 5). When the Laplacian $\nabla^2\rho(\mathbf{r}_{BCP}) = L(\mathbf{r})$ is negative, the electron density is locally concentrated at the BCP, which in turn exerts a net attractive force on the nuclei of the bonded atoms (Figure 2). This can be used to distinguish between various types of interactions. Negative values of $L(\mathbf{r})$ are accompanied by high electron density at the BCP, which are commonly associated with a covalent character of the bond (shared interaction), while distinct positive values of $L(\mathbf{r})$ in connection with low electron density at the BCP are attributed to closed-shell interactions (for example, ionic, coordinative, metal–metal bonds).[14] However, it is well-known that this strict classification does not hold for very polar bonds but is well established to compare similar bonds among each other.[15] Additional information can be gained by the value of the bond ellipticity,[16] $\varepsilon(\mathbf{r}_{BCP}) = (\lambda_1/\lambda_2 - 1)$, where the two λ values are the eigenvalues of the Hessian matrix perpendicular to the bond vector; ε quantifies the deviation from rotational symmetry for a given bond density distribution. Such a deviation would, for instance, be expected for an aromatic π-bond. Another topological parameter to classify the type of a bond is $\eta(\mathbf{r}_{BCP}) = |\lambda_1|/\lambda_3$. The value of $\eta(\mathbf{r}_{BCP})$ is less than unity for closed-shell (ionic) interactions, and increases with bond strength and decreases with the ionic contribution in shared (covalent) interactions. Apart from performing a topological analysis we compared the electron density after multipole refinement to theoretical values [in squared brackets]. The latter values result from multipole refinement of calculated structure factors obtained from Fourier transform with the program TONTO[17] from a previously calculated single-point wave function (Gaussian[18] at the ωB97XD/6-311G(d,p) level).[9a,10] From this, multipole refinements against the theoretical data a local scattering factor database was generated with the program InvariomTool[19] (see the Experimental Section).

The isomer **1** crystallizes in the monoclinic space group $P2_1/n$ with the midpoint of the central silicon ring residing on an inversion center (Scheme 1). The asymmetric unit contains half a molecule and one benzene molecule as lattice solvent. The central motif of **1** consists of a tricyclic arrangement of silicon atoms in a chair conformation similar to the fully saturated compound previously reported by Kira et al.[11] Two of them are substituted by two Tip ligands, two by only one and two by none, only bound to three neighboring silicon atoms. At the latter we found a distinct valence shell charge concentration (VSCC) of −2.08 [−1.39] e Å^{-5} in the position where the lone pair of the silicon(0) atom would be expected (Si3; Figure 3) in the Lewis diagram. Formally one could assign the oxidation state + II to Si1, + I to Si2 and zero to Si3. We found a similar pattern of + 1.6 e [+ 1.4 e], + 0.6 e [+ 0.6 e], −0.3 e [−0.1 e], respectively from the Bader charges obtained by integration of the atomic basins. This documents a good agreement of experiment and theory. The different charges indicate that polarization in the silicon ring occurs: the higher electronegativities of the adjacent carbon atoms suggest a polarization especially of the Si–C bonds. The values of $\rho(\mathbf{r})$ at the BCP of the Si1–Si2 and Si1–Si3 bonds are similar with 0.537(5) [0.524] and 0.545(6) [0.518] e Å^{-3}, respectively, whereas the transannular Si2–Si3 bond however accumulates only 0.466(7) [0.484] e Å^{-3}. The highest value of $\rho(\mathbf{r}_{BCP})$ is found between the Si2-Si3′ silicon atoms with 0.595(11) [0.537] e Å^{-3}. The same is valid for the $L(\mathbf{r})$ values. Between Si1–Si2 and Si1–Si3 $L(\mathbf{r})$ is similar with −1.645(8) [−1.798] e Å^{-5} and −1.628(8) [−1.616] e Å^{-5}, respectively, while the transannular Si2–Si3 bond shows a much higher $L(\mathbf{r})$ value of −1.164(9) [−0.940] e Å^{-5}. The most negative $L(\mathbf{r})$ for a Si–Si bond in **1** was found for the Si2–Si3′ bond, with −2.285(12) [−1.798] e Å^{-5}. The qualitative comparability of the $L(\mathbf{r})$ distribution is remarkably good, except for Si1–Si3 (Figure 2; Supporting Information, Figure SI16). In any case, the weakest interaction is the transannular bond between Si2 and Si3, the strongest is at the outside of the four-membered ring between Si2′ and Si3 accommodating the π-bond in the Lewis diagram, and the Si1–Si3 single bond in the three-membered ring lies half-way in between.

Importantly, no BCP was found for a possible through-space interaction between Si3 and Si3′. The triangle formed by Si1-Si2-Si3 (Figure 1) is a typical example of strained ring systems with bent bonds.[13,20] The maxima in the deformation density are clearly outside of the line directly connecting the atoms and the bond paths are extremely curved (Figure 5). In contrast to the covalent silicon–silicon bonds, the silicon–carbon bonds are much more polar (Supporting Information, Figure SI15). Close to the silicon atom, $L(\mathbf{r})$ reaches a high

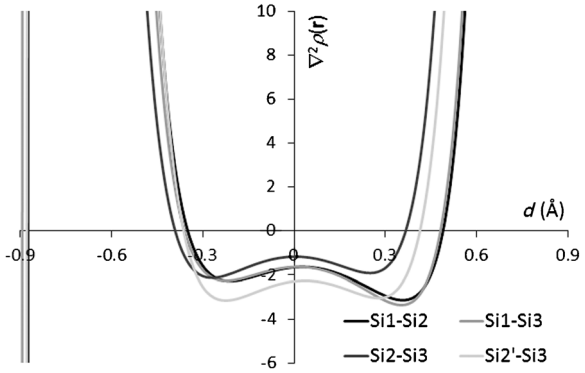

Figure 2. $L(\mathbf{r})$ along selected bond paths in **1**.

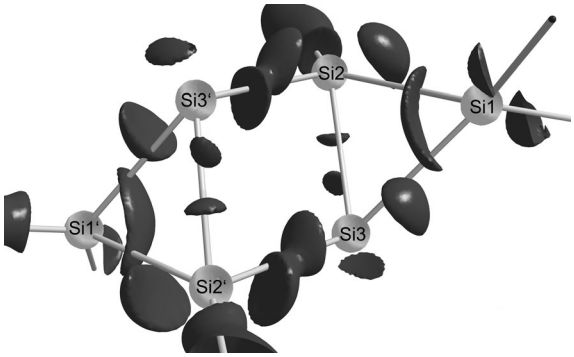

Figure 3. Laplacian distribution around the silicon atoms of **1** at an isosurface level of −1.9 e Å^{-5}. Si3–Si3′ distance: 2.70638(16) Å.

maximum around + 600 e Å^{-5} and decreases to almost zero at the BCP with a plateau of slightly negative values and reaches a minimum close to the carbon atoms. This distribution can be attributed to the strongly polar character of these bonds. The distribution of $L(\mathbf{r})$ also explains the differences of the value at the BCP between experiment and theory.

The ionic character of the Si–C bonds is also obvious for the $\eta(\mathbf{r}_{BCP})$ value at the BCPs (Supporting Information, Table SI8). While $\eta(\mathbf{r}_{BCP})$ is around one or higher for the Si–Si bonds, thus indicating their covalent character, $\eta(\mathbf{r}_{BCP})$ is below 0.5 for the Si–C bonds, demonstrating their high ionic character. The Si–C bonds in **1** exhibit similar properties to Si–C, Si–N, and Si–O bonds previously analyzed.[15e,21]

The second isomer of hexasilabenzene **2** crystallizes in the space group *C*2/*c* with Si1 and Si4 on a twofold rotational axis (Scheme 1). The asymmetric unit contains half a molecule and 1.5 THF molecules. The bridged propellane-like **2** adopts a cage structure consisting of six silicon atoms. As in **1**, two vertices are substituted by two Tip ligands, two by one and two by none, but bound to just three silicon atoms. In contrast to the carbon-based [1.1.1]propellane, there is no accumulation of electron density (Figure 1, right) and no indication of a Si–Si bond path between the bridgehead atoms Si3···Si3′ at the hub of the silapropellane moiety.[22] As in **1**, there is a distinct VSCC in the non-bonding region of Si3 (−4.00 [−1.15] e Å^{-5}) pointing away from the inner silicon cage, in line with the expectation derived from the simple Lewis formalism and an alternative description as a charge shift bond (Figure 4).[23] The non-existence of a bridgehead bond

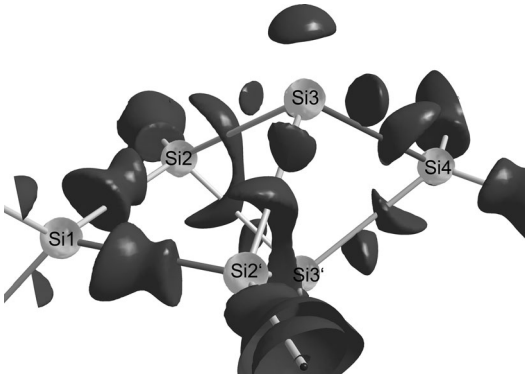

Figure 4. Laplacian distribution around the silicon atoms of **2** at an isosurface level of −1.9 e Å^{-5}. Si3–Si3′ distance: 2.64173(12) Å.

path confirms the substantial biradical character, but the closeness of the ring critical point to the potential bond critical point also confirms that even only slight differences in the density of these systems can create or prevent a bridgehead bond path.[24]

As the conformational change **1**→**2** would not require any ligand scrambling in the cage structure **2**, the expected oxidation states of the silicon atoms are + II for Si1 and Si4, + I for Si2, and zero for Si3, as in **1**. We retrieved the pattern in the experimental Bader charges but found a slight difference in the theoretical data. Si1 and Si4 differ clearly in their experimentally derived value of 1.06 [1.45] e (Si1) and 1.55 [1.41] e (Si4). In fact, the differing charges are in better agreement with experiment than the theory. Atoms Si1 and Si4 show different reactivity in **2**, which was recently reported.[25] We currently cannot explain this discrepancy. However the high integrated charge of Si4 also fits the unusual downfield resonance of $\delta = 174.6$ ppm in the ^{29}Si NMR spectrum of **2** described earlier, which can be rationalized by invoking magnetically induced cluster currents.[10] Atoms Si2 and Si3 show much lower Bader charges (+ 0.73 [+ 0.64] and −0.30 [−0.15]). The electron density values at the BCP of the Si1–Si2 bond are, upon conversion from **1** to **2**, the highest values in **2**, with 0.580 [0.575] e Å^{-3}, followed by Si2–Si3′ and Si2–Si3, with 0.555 [0.538] and 0.512 [0.532] e Å^{-3}, respectively. The Si3–Si4 bond lies in between, with 0.527 [0.519] e Å^{-3}. In terms of bond strength, this picture is consistent with $L(\mathbf{r})$ at the BCP. Si1–Si2 has the strongest shared interaction with −2.942 [−2.580] e Å^{-5} and the other BCPs show a much lower level of around −1.8 e Å^{-5}, with the weakest interaction being the Si2–Si3 bond (Figure 5).

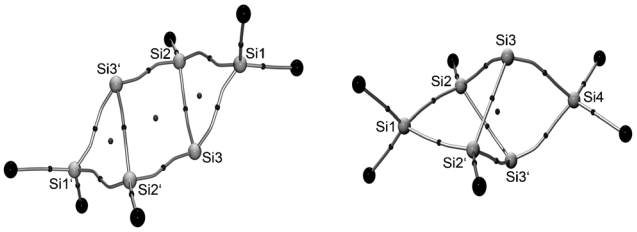

Figure 5. Curved bond paths with bond critical points and ring critical points for **1** (left) and **2** (right).

The qualitative shapes of the $L(\mathbf{r})$ curves in **2** are comparable to **1**, but look more alike among each other. The silicon–carbon bonds in **2** also show the strong polarization towards the carbon atoms (Supporting Information, Figure S19) with a low η value and thus high ionic contribution.[15e,21b] The ε values along the BP in **2** have a similar distribution as in **1** along the Si–C bonds while Si2–C16 and Si4–C31 differ most prominently from the theoretical values (see the Supporting Information). This is consistent with the deviation of ε in the Si2–Si3 and the Si3–Si4 bond where the deviation is also most prominent. The overall qualitative comparability of ε in **2** is much better than in **1** and the ellipticities are higher. The ellipticity of the Si1–Si2 bond is remarkably low while the bonds of the silapropellane residue are distinctly higher. This fits the observation that the silapropellane part of **2** also shows bent bonds as can be seen in Figure 1, right. The remaining silapropellane wings and the bridging bonds to Si1 are depicted in the Supporting Information, Figure S27.

Comparing **1** and **2**, both cores can be imagined as positively charged metal cages of silicon atoms that are not strongly polarized in themselves and are coordinated by negatively charged carbon atoms. The Si–Si bonds are quite similar in strength, except for the considerably weaker transannular Si2–Si3 bond in **1**, lending further support to the delocalized nature according to the simple resonance structures of Scheme 1. The Si1–Si2 bond is stronger and less

elliptic; it accommodates less delocalized electron density than the others. The distribution of $L(\mathbf{r})$ along the Si–Si BPs does not differ much in absolute value but the experimental values have a tendency to polarize in the direction of Si3. The theoretical distribution is more symmetric. Even though the absolute values are different in theory and experiment, the qualitative ε values of the Si–Si bonds suggest a more delocalized electron density distribution in **2**, although the bond lengths are in the range of single bonds in the propellane part of the molecule and the bridging Si1 being more sigma bonded to its adjacent silicon atoms (Supporting Information, Figure S17).

In conclusion, our experimental charge density investigation shows that the assumption of aromaticity in the ring isomer of hexasilabenzene **1** is valid. Clearly there is a VSCC present in the non-bonding region in the apical position of Si^0. Furthermore, the transannular VSCCs of opposite silicon atoms indicate the presence of two transannular bonds. A discussion of bond distances from independent atom model refinement alone is insufficient, because all Si–Si distances are similar. An interstitial bond between both Si^0 bridgehead atoms in the cage silapropellane conformer **2** was not found, although it is present in the similarly arranged carbon propellane. It is interesting to note that the Bader charges correlate well with the three different oxidation states of the silicon atoms and even respond to the chemically different environment in **2**.

Experimental Section

The high-resolution X-ray data for the multipole refinements were collected from oil-coated shock-cooled crystals selected using the X-Temp2 device[26] on a BRUKER Smart APEX II Ultra with INCOATEC mirror optics (Mo-Kα radiation, $\lambda = 0.71073$ Å) equipped with a Bruker liquid nitrogen cooling device.

Crystal data for **1**: $C_{102}H_{150}Si_6$, $M = 1544.76\ g\,mol^{-1}$, monoclinic space group $P2_1/n$, $a = 12.644(2)$, $b = 26.368(5)$, $c = 15.206(3)$ Å, $\beta = 107.183(3)°$, $V = 4843.3(16)$ Å^3, $Z = 2$, $\rho_{calcd} = 1.059\ Mg\,m^{-3}$, $\mu = 0.129\ mm^{-1}$, 731646 reflections measured, 55651 unique, $R1(I>2\sigma(I)) = 0.0299$, $wR2(I>2\sigma(I)) = 0.0643$ $GoF = 2.226$ after multipole refinement. Crystal data for **2**: $C_{102}H_{162}O_3Si_6$, $M = 1604.86\ g\,mol^{-1}$, monoclinic space group $C2/c$, $a = 21.505(6)$, $b = 17.375(5)$, $c = 25.979(7)$ Å, $\beta = 94.554(10)°$, $V = 9676.3(5)$ Å^3, $Z = 2$, $\rho_{calcd} = 1.102\ Mg\,m^{-3}$, $\mu = 0.134\ mm^{-1}$, 618471 reflections measured, 55022 unique, $R1(I>2\sigma(I)) = 0.022$, $wR2(I>2\sigma(I)) = 0.056$, $GoF = 2.63$ after multipole refinement. The data collection strategy for **1** and **2** was calculated with COSMO to ensure high redundancy and completeness up to full resolution. Data reduction was performed with SAINT and absorption correction with SADABS. The promolecule was refined with SHELXL97[27] and ShelXle.[28] Multipole refinement was completed with XD2006[29] and MolecoolQT.[30] CCDC 915313 (**1**) and 915312 (**2**) contain the supplementary crystallographic data for this paper. These data can be obtained free of charge from The Cambridge Crystallographic Data Centre via www.ccdc.cam.ac.uk/data_request/cif

Before the properties of **1** and **2** could be analyzed, some inherent structural problems had to be overcome. Large molecules in the solid state are nearly always disordered,[31] which reduces the scattering power of X-ray radiation and thus the resolution of the measurement drastically.[32] Furthermore, the treatment of disordered structures in experimental X-ray charge density analysis is not a common task. Luckily the crystals of **1** and **2** showed enough scattering power for charge density analysis with in-house measured data despite the disorder of the solvent molecules and parts of the ligand sphere of **1** and **2**. The multipole model, used for refinement of both structures, was not designed to model the charge density of disordered structures.[28] Nevertheless, a good approximation of the electron density in these disordered regions was achieved by using theoretically derived scattering factors from a tailor-made database of those chemical environments that occur in the two structures with the program InvariomTool.[19] This procedure is related to the invariom approach.[19] We still claim to have performed an experimental charge density study, because the multipole parameters describing the molecular core were freely refined and only those for the disordered outer sphere were held fixed (see also the Supporting Information).

Received: December 11, 2012
Revised: January 22, 2013
Published online: March 14, 2013

Keywords: bent bonds · charge density · cluster compounds · QTAIM calculations · silicon

[1] R. West, M. J. Fink, J. Michl, *Science* **1981**, *214*, 1343 – 1344.
[2] M. Weidenbruch, S. Willms, W. Saak, G. Henkel, *Angew. Chem.* **1997**, *109*, 2612 – 2613; *Angew. Chem. Int. Ed. Engl.* **1997**, *36*, 2503 – 2504.
[3] a) P. von R. Schleyer, *Chem. Rev.* **2001**, *101*, 1115 – 1117; b) P. von R. Schleyer, *Chem. Rev.* **2005**, *105*, 3433 – 3435; c) E. Matito, J. Poater, M. Sola, P. von R. Schleyer, *Aromaticity and Chemical reactivity* (Eds.: P. K. Chattaraj), Taylor and Francis/CRC, Boca Raton, **2009**, pp. 419 – 438.
[4] a) G. Raabe, J. Michl, *The Chemistry of Organosilicon Compounds* (Eds.: S. Patai, Z. Rappoport), Wiley, New York, **1989**, pp. 1102 – 1108; b) Y. Apeloig, M. Karni, *The Chemistry of Organosilicon Compounds* (Eds.: S. Patai, Z. Rappoport), Wiley, New York, **1989**, pp. 151 – 166; c) A. G. Brook, M. A. Brook, *Adv. Organomet. Chem.* **1996**, *39*, 71 – 158; d) P. von R. Schleyer, H. Jiao, N. J. R. van Eikema Hommes, V. G. Malkin, O. L. Malkina, *J. Am. Chem. Soc.* **1997**, *119*, 12669 – 12670; e) *The Chemistry of Organosilicon Compounds*, *Part II* (Eds.: Y. Apeloig, Z. Rappoport), Wiley, New York, **1998**; f) K. K. Baldridge, O. Uzan, J. M. L. Martin, *Organometallics* **2000**, *19*, 1477 – 1487.
[5] K. Wakita, N. Tokitoh, R. Okazaki, S. Nagase, *Angew. Chem.* **2000**, *112*, 648 – 650; *Angew. Chem. Int. Ed.* **2000**, *39*, 634 – 636.
[6] Y. Kabe, K. Ohkubo, H. Ishikawa, W. Ando, *J. Am. Chem. Soc.* **2000**, *122*, 3775 – 3776.
[7] a) R. Kinjo, M. Ichinohe, A. Sekiguchi, N. Takagi, M. Sumimoto, S. Nagase, *J. Am. Chem. Soc.* **2007**, *129*, 7766 – 7767; b) H.-X. Yeong, H.-W. Xi, K. H. Lim, C.-W. So, *Chem. Eur. J.* **2010**, *16*, 12956 – 12961.
[8] a) S. S. Sen, H. W. Roesky, K. Meindl, D. Stern, J. Henn, A. C. Stückl, D. Stalke, *Chem. Commun.* **2010**, *46*, 5873 – 5875; b) J. S. Han, T. Sasamori, Y. Mizuhata, N. Tokitoh, *Dalton Trans.* **2010**, *39*, 9238 – 9240.
[9] a) K. Abersfelder, A. J. P. White, H. S. Rzepa, D. Scheschkewitz, *Science* **2010**, *327*, 564 – 566; b) R. J. F. Berger, H. S. Rzepa, D. Scheschkewitz, *Angew. Chem.* **2010**, *122*, 10203 – 10206; *Angew. Chem. Int. Ed.* **2010**, *49*, 10006 – 10009.
[10] K. Abersfelder, A. J. P. White, R. J. F. Berger, H. S. Rzepa, D. Scheschkewitz, *Angew. Chem.* **2011**, *123*, 8082 – 8086; *Angew. Chem. Int. Ed.* **2011**, *50*, 7936 – 7939.
[11] T. Iwamoto, K. Uchiyama, C. Kabuto, M. Kira, *Chem. Lett.* **2007**, *36*, 368 – 369.
[12] N. K. Hansen, P. Coppens, *Acta Crystallogr. Sect. A* **1978**, *34*, 909 – 921.
[13] R. F. W. Bader, *Atoms in Molecules—A Quantum Theory*, Oxford University Press, New York, **1990**.

[14] a) P. Coppens, *X-Ray Charge Densities and Chemical Bonding*, Oxford University Press, Oxford, **1997**; b) D. Stalke, *Chem. Eur. J.* **2011**, *17*, 9264 – 9278; c) U. Flierler, D. Stalke, L. J. Farrugia, *Modern Charge-Density Analysis* (Eds.: C. Gatti, P. Macchi), Springer, Heidelberg, **2012**, S. 435 – 467; d) "Electron Density and Chemical Bonding I (Experimental Charge Density Studies) and II (Theoretical Charge Density Studies)" in *Struct. Bonding*, *Vol.* 146 (Ed.: D. Stalke), Springer, Berlin, **2012**.

[15] a) D. Leusser, B. Walfort, D. Stalke, *Angew. Chem.* **2002**, *114*, 2183 – 2186; *Angew. Chem. Int. Ed.* **2002**, *41*, 2079 – 2082; b) S. L. Hinchley, P. Trickey, H. E. Robertson, B. A. Smart, D. W. H. Rankin, D. Leusser, B. Walfort, D. Stalke, M. Bühl, S. J. Obrey, *J. Chem. Soc. Dalton Trans.* **2002**, 4607 – 4616; c) D. Leusser, J. Henn, N. Kocher, B. Engels, D. Stalke, *J. Am. Chem. Soc.* **2004**, *126*, 1781 – 1793; d) N. Kocher, D. Leusser, A. Murso, D. Stalke, *Chem. Eur. J.* **2004**, *10*, 3622 – 3631; e) N. Kocher, C. Selinka, D. Leusser, D. Kost, I. Kalikhman, D. Stalke, *Z. Anorg. Allg. Chem.* **2004**, *630*, 1777 – 1793; f) J. Henn, D. Ilge, D. Leusser, D. Stalke, B. Engels, *J. Phys. Chem. A* **2004**, *108*, 9442 – 9452; g) M. S. Schmøkel, S. Cenedese, J. Overgaard, M. R. V. Jørgensen, Y.-S. Chen, C. Gatti, *Inorg. Chem.* **2012**, *51*, 8607 – 8616; h) D. Stalke, *Chem. Commun.* **2012**, *48*, 9559 – 9573.

[16] J. R. Cheeseman, M. T. Caroll, R. F. W. Bader, *Chem. Phys. Lett.* **1988**, *143*, 450 – 458.

[17] D. Jayatilaka, D. J. Grimwood, *Comput. Sci. ICCS* **2003**, *4*, 142 – 151.

[18] Gaussian 09 (Revision C.01), M. J. Frisch et al. (see the Supporting Information), Gaussian, Inc., Wallingford CT, **2010**.

[19] B. Dittrich, T. Koritsanszky, P. Luger, *Angew. Chem.* **2004**, *116*, 2773 – 2776; *Angew. Chem. Int. Ed.* **2004**, *43*, 2718 – 2721.

[20] a) C. A. Coulson, W. E. Moffitt, *J. Chem. Phys.* **1947**, *15*, 151; b) T. Koritsanszky, J. Buschmann, P. Luger, *J. Phys. Chem.* **1996**, *100*, 10547 – 10553; c) M. Messerschmidt, S. Scheins, L. Grubert, M. Pätzel, G. Szeimies, C. Paulmann, P. Luger, *Angew. Chem.* **2005**, *117*, 3993 – 3997; *Angew. Chem. Int. Ed.* **2005**, *44*, 3925 – 3928.

[21] a) K. L. Geisinger, M. A. Spackman, G. V. Gibbs, *J. Phys. Chem.* **1987**, *91*, 3237 – 3244; b) W. Scherer, P. Sirsch, D. Shorokhov, G. S. McGrady, S. A. Mason, M. G. Gardiner, *Chem. Eur. J.* **2002**, *8*, 2324 – 2334; c) G. V. Gibbs, A. E. Whitten, M. A. Spackman, M. Stimpfl, R. T. Downs, M. D. Carducci, *J. Phys. Chem. B* **2003**, *107*, 12996 – 13006; d) Y. Yang, *J. Phys. Chem. A* **2010**, *114*, 13257 – 13267.

[22] D. Nied, R. Köppe, W. Klopper, H. Schnöckel, F. Breher, *J. Am. Chem. Soc.* **2010**, *132*, 10264 – 10265.

[23] W. Wu, J. Gu, J. Song, S. Shaik, P. C. Hiberty, *Angew. Chem.* **2009**, *121*, 1435 – 1438; *Angew. Chem. Int. Ed.* **2009**, *48*, 1407 – 1410.

[24] a) F. Breher, *Coord. Chem. Rev.* **2007**, *251*, 1007 – 1043 and references therein; b) R. F. W. Bader, T. T. Nguyen-Dang, *Rep. Prog. Phys.* **1981**, *44*, 893 – 905.

[25] K. Abersfelder, A. Russell, H. S. Rzepa, A. J. P. White, P. R. Haycock, D. Scheschkewitz, *J. Am. Chem. Soc.* **2012**, *134*, 16008 – 16016.

[26] a) T. Kottke, D. Stalke, *J. Appl. Crystallogr.* **1993**, *26*, 615 – 619; b) D. Stalke, *Chem. Soc. Rev.* **1998**, *27*, 171 – 178.

[27] G. M. Sheldrick, *Acta Crystallogr. Sect. A* **2008**, *64*, 112 – 122.

[28] C. B. Hübschle, G. M. Sheldrick, B. Dittrich, *J. Appl. Crystallogr.* **2011**, *44*, 1281 – 1284.

[29] a) A. Volkov, P. Macchi, L. J. Farrugia, C. Gatti, P. R. Mallinson, T. Richter, T. Koritsanszky, XD2006, **2006**; b) T. S. Koritsanszky, P. Coppens, *Chem. Rev.* **2001**, *101*, 1583 – 1627.

[30] C. B. Hübschle, B. Dittrich, *J. Appl. Crystallogr.* **2011**, *44*, 238 – 240.

[31] K. Meindl, J. Henn, N. Kocher, D. Leusser, K. A. Zachariasse, G. M. Sheldrick, T. Koritsanszky, D. Stalke, *J. Phys. Chem. A* **2009**, *113*, 9684 – 9691.

[32] D. Watkin, *J. Appl. Crystallogr.* **2008**, *41*, 491 – 522.

